RSC Advances

ROYAL SOCIETY OF CHEMISTRY

www.rsc.org/advances

Fabrication and evaluation of polymer-based esophageal stents for benign esophagus stricture insertion

Tianwen Yuan[a,b†], Reila Zheng[a†], Jia Yu[a], Laura Edmonds[a], Wei Wu[c], Jun Cao[d], Fei Gao[e], Yueqi Zhu[b]*, Yingsheng Cheng[b]* and Wenguo Cui[a]*

[a] Orthopedic Institute, College of Medicine, Soochow University, 708 Renmin Road, Suzhou, Jiangsu 215006 , P. R. China.

[b] Department of Radiology, The Sixth Affiliated People's Hospital, Medical School of Shanghai Jiao Tong University, No. 600, Yi Shan Road, Shanghai, 200233, P.R.

[c] Department of general surgery, Yangzhou First Hospital Affiliated to Southeast University, 365 Hanjiang Middle Road, Yangzhou, Jiangsu 225000, P. R. China.

[d] Department of Interventional oncology, Dahua Hospital, Xuhui District, Shanghai 200237, China.

[e] Zhejiang Zylox Medical Device co., Ltd, No. 1500, Wenyi west Road, Hangzhou, Zhejiang, 311121, P. R. China.

† These authors contributed equally to this work.

* Correspondence: wgcui80@hotmail.com (W.C);

chengyingshengradio@hotmail.com (Y.C); zhuyueqi@hotmail.com (Y. Z);

Tel./Fax.: +86-512-67781420.

Abstract: In benign esophageal strictures, an esophageal stent implantation can relieve esophageal lesions caused by esophageal stenosis and obstruction. However, the removals of metallic stents are difficult and biodegradable polymer stents show the poor mechanical properties. In this study, polypropylene lines as skeleton fibers and silicone as coating membranes were chosen to knit an esophageal stent for improved structural strength and easy removal. The mechanical testing demonstrated that the stent maintained its original mechanical characteristics after two hundred repeated compressions and pulls. According to the finite element simulation analysis of the stent, the left and right sides had higher stress concentrations as the loading contact site and the restrain site of the both ends. The proliferation of the smooth muscle cells showed no signs of cell toxicity. During the in vivo evaluation, the changes to the esophageal wall were significant; thinner epithelial and smooth muscle actin layers in the PP-silicone stent group than in the control group ($P < 0.05$). Esophageal injury and collagen deposition following the stent insertion were similar to the control group ($P > 0.05$). The esophageal PP-silicone stent insertion was feasible and provided reliable support for at least 4 weeks, with acceptable migration rates and without causing severe injury or collagen deposition. Therefore PP-stents have great potential to provide a new method and practical basis for the treatment of benign esophageal stricture.

Keywords: Benign esophageal stricture; esophageal stent; silicon membrane; polypropylene;

Introduction

Esophageal benign stricture is the pathological stricture caused by any disease in the esophageal antrum, including infections, surgery, trauma, burns, and other benign stricture. In addition, the external pressure of the mucosal ring and the mediastinal tissue can also cause esophageal stricture. Benign stricture of the esophagus (BSE) can severely reduce quality of life and cause major complications such as aspiration, weight loss and malnutrition.[1] Esophageal stent implantation has been widely used in clinical practice and can relieve benign and malignant lesions caused by esophageal stenosis and obstruction. This surgical method effectively alleviates patients with dysphagia and has excellent treatment results, few instances of trauma, quick recovery, low cost, simple operation safety and other advantages. Clinical research confirmed that esophageal stent implantation for esophageal benign stricture can achieve satisfactory results. [2-4]

With the development of materials technology, metal and polymer stents are now the most widely used stents in esophageal benign stricture. Metal stents have been widely used in clinical applications because of their high strength and structural stability. Song et al. originally designed the stainless steel coated stent and later, the nickel-titanium alloy stent which in a series of studies achieved good results.[5,6] Cheng et al. also used a nickel-titanium alloy temporary stent with a membrane covering it in the treatment of esophageal benign stricture and cardia achalasia patients. [7] The mid-long-term efficacy analysis found that this stent performed better in the long-term compared to balloon dilation and permanent stents in the treatment of benign stricture. Metal stents can demonstrate a very good expansion of structure, mechanical performance, and reduce restenosis, stent migration, aspiration pneumonia, and tracheosophageal leakage. However, due to the high strength and rigidity of metals, the stent is not easy to remove. Forcible removal causes pain, perforation, bleeding, and strong foreign body reaction and complications.[8] Thus metal stent implantation still faces many challenges and there is a clinical need to overcome these shortcomings.

On the other hand, the polymer polylactic acid (PLA) materials have good flexibility and high tensile strength. Braided stent PLA materials demonstrate lower rates of tissue injury, smaller foreign body reactions, fewer polyps at both ends of the bracket and lower rates of bleeding, and other complications compared to metal stents. Thus it is hopefully put into extensive use in esophageal stent domain. There

are many pieces of literature that describe treatment of esophageal stricture, esophageal fistula, and postoperative anastomotic fistula. [9-13] However, this polymer materials stent's outstanding problem is that mechanical expansion is poor and can easily lead to the displacement and obstruction. [14-16]

Currently polymer esophageal stents mainly consist of polymer membrane-coated metal stents, which takes advantage of the mechanical performance of metal stents, and a layer of polymer coating on the outside which improves the implantation and removal procedure.[17] However, there are still complications such as pain, perforation, bleeding and strong foreign body reaction caused by metal wire removal. Presently, stents with polymer skeletons are mainly in research, such as the use of PLA wire knitted into the esophagus stent. Controlling the biodegradablility of PLA can eliminate the need of stent removal.[18] However, the mechanical properties of a PLA stent are poor, and it is easy to slip, translocate, and obstruct after implantation, which is not conducive to the clinical application of stents.[19] Based on existing polymer materials, we developed a stent with high mechanical support strength, fixed in position, which combines the advantages of metallic stents and polymer stents. We expect these stent could improve expansion, fixation, and ease of removal, and most of all does not affect the normal esophageal peristalsis and esophageal function during the recovery of the lesion.

Polypropylene (PP) yarn has high mechanical strength.[20] The crystallinity of PP threads affects its rigidity and its flexibility prevents damage to the surrounding tissues.[21] By considering the properties of the esophageal stent skeleton and membrane, we selected PP as a skeleton fiber for a knitted esophageal stent mould with biological medical silicone coating the stent surface. We integrate the highly expansible PP and biocompatibility of silicone in the design of our esophageal stent. We inserted the PP-silicone stents into the normal esophagus of rabbits to determine the feasibility of this technique and observe the in vivo tissue reaction after stent insertion. At the same time the mechanical properties and safety of the system were investigated in this paper.

Materials and Methods

Materials and animals

PP lines composed of 0.25 mm diameter fibers (density 76 g/m^2) were obtained from Covidien (Trevoux, France). The committee which is in charge of all animal

researches of our institute authorized every protocols, which were conducted in accordance with the guidelines of the International Council on Animal Care (US National Institutes of Health and European Commission). Fifteen New Zealand rabbits of both sexes that were 5-8 months old were randomized divided into a 1-week (n=5) and 4-week (n=5) PP-silicon stent insertion group and a Control group (n=5) that did not receive any intervention. Rabbits in the PP-silicone stent groups received stent insertion into the lower 1/3 of the esophagus under fluoroscopic guidance. All rabbits underwent esophagography before stent insertion, and at 1-week and 4-week follow-up.

PP stents description

The PP stent used in this study consists of three parts: a polypropylene fiber as framework, a biomedical silicone gel membrane, and a stent delivery system. The stent is knitted from a 0.25 mm diameter polypropylene fiber wire, knotted on the 10mm diameter metal mandril with a single fiber knit. The density of the fiber cross distribution, the height and the knit angle of the stent had been designed basing on the model. After the framework was knitted, the braided fabric which covered the metal mandril was dipped into silicone gel solutions. This liquid silicone rubber C6-530 (Dow Corning Inc.) was used for the silicone gel membrane. C6-530 is a heat cured elastomer raw material for customers to fabricate medical devices and parts. The knitted framework can then be coated with a biomedical silicone gel membrane layer to solidify the stent. This was repeated five times and the stent was then placed into an oven for thermoforming at a constant temperature for 12 hours at 80 ^{o}C. Thermoforming fixes the shape of fiber interior structure or braided fabric and maintains the size. Thus this process ensures the fabric shape and function will remain stable after withdrawn from the metal mandril. [22]

The stent consists of a self-expanding, cross-linked polypropylene fiber cylindrical mesh body with a 15-mm cydariform and tubiform at its head and distal ends to prevent stent migration at the gastroesophageal junction. The stent body and the tubiform tail were covered with a silica gel membrane. The diameter of the main body of the stent body increases to 10 mm, and the total stent length is 25 mm when fully expanded. There is a trisection of anti-reflux valve attached at the connection part of the stent body and the tail. An corrosion-resistant coating was applied on stent wires to avoid the damage from acidic gastric juice. Each stent was

compressed and deployed by an 8 mm (~24Fr) delivery system, and the whole stent body was radiopaqued under the fluoroscope to facilitate accurate positioning.

Stent radial force test

The radial forces of the stent were detected for the resist extrusion performance and radial direction braced force support. Measurements of the radial forces were obtained by a direct measurement of the stent's compression between a pressure head (5 mm/in width, with a 0.1 mm/s and a flat plate using the Instron 5272 Advanced Materials Testing System (Instron Corporation, Norwood, Massachusetts, USA). The radial force curves represented the stability of the stent against potential outer radial forces. This test had been done two hundred times.

For the stent support section tensile test, the longitudinal side of the stand is cut and the two ends of the fixed shear plane are fixed. The maximum strength of the tensile strength of the stent is then determined. The tensile curves describe the maximum tensile force that the material can withstand. This test had been done one hundred times.

Finite element modeling

A finite element model of the frame was established to match the structure and size of the experimental stent. The model simulates the structure of the braided knit and the outer membrane. The braided structure using the automatic programming interface of the SolidWorks 2003 CAD software was set-up for implement a self-defined structure of geometry modeling. Then by using the HyperMesh software, the gridding and meshing was completed. The elements are hexahedral elements (C3D8I) with the average element size being about 0.3mm×0.1mm×0.1mm. The outer membrane was established in ABAQUS v6.13 software, using shell elements (S4R) division with a size of 0.5 mm and then assembled together. There are 18368 in total elements in the model. The knit structure and the outer membrane are attached to each other. The materials of stent are all simplified as linear elastic types. The Young's modulus of the braided stent and covered outer membrane is 1000 MPa and 3000MPa respectively with the Poisson ratio being 0.45 and 0.38 respectively. The bottom of the ends of model are fully constrained. The middle of the model is applied perpendicular direction of compression by used in the rigid cube, and compression deformation displacement is about 1.5mm (15%).

Cell culture

SMCs, isolated from a rat aorta pectoralis, were grown in the culture medium in a humidified 5% CO_2 incubator at 37 ^{o}C. SMCs were identified with the expression of anti-smooth muscle actin and their typical elongated, swirling, and over lapping morphology. The cells were seeded at a density of 1×10^4 cells per well in a12-well plate and incubated for 24 h. The PP-silicon was dipped in the culture medium. These cells were then cultured for another 9 days. Proliferation of the cells was observed using a CCK-8 assay for cell counting (Cell countingkit-8, Dojin do, Kumamoto, Japan). 100 mL of the incubated medium was pipetted into a 96-well plate and the absorbance at450 nm was measured using a microplate reader (Thermo LabSystems, Helsinki, Finland).

Stent insertion

The subject group consisted of 15 healthy New Zealand rabbits that were between the ages of 5 and 8 months old. Both sexes of rabbit were tested and the weight varied from 2.3-3.8kg. The rabbits were randomly divided into a stent group and a 1-week (n=5) and 4-week (n=5) PP-silicon stent insertion group and a control group (n=5) that did not receive any intervention. Rabbits in the PP-silicone stent groups underwent PP-silicone stent placement in the lower third of the esophagus. A 0.035-inch diameter, 260-cm long, stiff exchange wire (Terumo, Tokyo, Japan) was inserted through the mouth and into the stomach under fluoroscopic guidance. The stent-delivery system was introduced over the guidewire until it reached the lower third of the esophagus. The stent was then released, based on esophagographic images obtained under fluoroscopic guidance. A balloon catheter (10 × 40 mm) was inflated within the stent to achieve full stent expansion. The implementation of duplicating esophagography was applied in order to ensure the extension level of stent and eliminate esophageal perforation. Stent insertion did not appear on the animals in comparison group.

Histological examination

Five animals in each group were euthanized at each time point to compare tissue reactions. The inserted stent was carefully removed from the resected esophageal sample. The inserted stent was carefully removed from the resected esophageal sample. The sented and comparison esophageal samples passed through a series of graded ethanol solutions (70% to 100%) and embedded in paraffin. Serial paraffin-embedded, esophageal cross-sections were stained with hematoxylin and eosin (HE) to evaluate the inflammation reaction.[1] Masson trichrome staining was used to assess submucosal collagen deposition. Mouse anti-proliferating cell nuclear antigen (PCNA) antibody (1:100 dilution) was used to immunostain esophageal samples by elivision immunohistochemical method. Negative controls were prepared by omitting the primary antibodies. The pathologist who reviewed the specimens and performed the analysis was blinded to the animal randomization, treatment procedures and follow-up protocols. The proliferation index was defined as the percentage of PCNA-positive cells divided by the total number of nucleated cells in the epithelial lining. The proliferation index of the submucosal layer occupied by the α-actinpositive area was assessed. The percentage of positive cells and the collagen area percentage were calculated using Image-Pro® Plus version 6.0 software (Media Cybernetics, Bethesda, Maryland, USA) in at least 20 randomly selected high-power (×400) tubulointerstitial fields from each section. Each specimen was cut into three uniform segments (both ends and middle) and there were five sets of segments for a total of fifteen segments. A pathologist selected the two best pieces from the series and conducted an image analysis.

Statistical analysis

The data analyzed in this experiment was obtained in triplicate. The data is expressed as mean value with standard deviations (SD). One-way ANOVA was used to compare the PCNA proliferation index, smooth muscle a-actin positive area, epithelial layer and collagen thickness in submucosa at each follow-up.

Results

Macro structure and clinical usability

The analysis of the material structure and clinical performance (Fig. 1) show perfect opened bare stents landscape and profile as well as related data parameters. The stent consists of a cylindrical, self-expanding, cross-linked polypropylene fiber mesh body with a 15 mm cydariform and 5 mm tubiform at its head and distal ends to prevent stent migration at the gastroesophageal junction. The stent body and the tubiform tail were covered with a silica gel membrane. The diameter of the main body of the stent body is 10 mm. The diameter of the stent head and distal end is 15 mm and the total stent length is 25 mm when fully expanded. There is a trisection of anti-reflux valve attached at the connection part of the stent body and the tail. Fig. 1 shows the external stent in the push and release map, and demonstrates the entire process of compression and release by an 8 mm (24 FR) delivery system. The stent shape was unchanged during and after fitting into and releasing, and demonstrated good elastic supporting forces.

Mechanical properties

To determine the mechanical properties, the tensile stress and strain for the PP stents were tested, and the results are shown in Fig. 2a and Fig. 2b. Mechanical analysis of the PP stent showed high tensile strength (nearly 6 MPa) and excellent tensile elongation (nearly 80%). The tensile strength of the supporting material can be seen (Fig. 2b). The tensile strength of the support section gradually rises until reaching a maximum tensile strength of 60 N before the material of the stent is torn apart. Supervene the tension gradually reduced. The PP stents displayed high elastic deformation with stent compression and spring-back while also being able to sustain strong tension forces. Over the testing processes, the stents were able to retain their elasticity after two hundred cycles of repeated compressions. The curves shown in Fig. 2a revealed that under the same compression rate, the compression load needed for the PP stent is nearly same. The curves shown in Fig. 2b revealed that under maximum tension, the tensile strength of the support material is also very similar. However the curves shown in Fig. 2a reveal that at the same compression rate of each stent, a stronger compression load and a lower spring-back displacement are needed for the stent. This data suggests that the PP material stent demonstrates high flexibility and elasticity.

Stress distribution of finite element analysis

The results showed that under the vertical compressive loading. The left and right sides of the stent were more obvious stress concentration as the loading contact site and the restrain site of the both ends (Fig. 3). The stress value of von Mises is about 25 MPa, the top contact stress is about 90 MPa, and the stress on the bottom supporting part is around 130 MPa. These values are all within the maximum range of the compression strength of the material. By compressive simulations on both sides of the stent, it can be clear that the in vivo strength of the stent mainly comes from both sides of the trumpet. Therefore the trumpet can be used as the buffer point of pressure. The tubular region of the stent is affected by the mechanical compression only after the trumpet has been compressed. The trumpet can play the dual role of being a fastening stent to prevent the stent from sliding and being a mechanical buffer at the same time.

In vitro stent evaluation

The smooth muscle (SMC) cells proliferation was measured using a colorimetric CCK-8 assay. SMC cells proliferation was recorded on these membranes after 1, 3, 6 and 9 days of culture. The cell culture plate was used as control. All results are summarized in Fig. 4. It is clear that the PP line, silicon membranes and PP-silicon groups show obvious cell proliferation at 6 and 9 days of culture. There is no significant difference ($P > 0.05$) in cell numbers between PP-silicon and control group, and between PP line and silicon membranes at 6 and 9 days of culture. This is indicative that the PP-silicon promotes SMC cell growth. Higher SMC cell proliferation rates are observed on PP line, silicon membranes and PP-silicon, and this phenomenon became obvious after 6 and 9 days of culture. The cytotoxicity of the stent material is scarcely observed from the results.

Intervention procedure

Stenting was successful in all 10 rabbits in the PP-silicone stent groups. All rabbits tolerated the procedure well and no animals died during the study. Procedure-related adverse events including esophageal perforation and bleeding, did not occur during or following stent insertion. No stent migration into the stomach

occurred after stent placement. Following stent insertion, contrast could pass smoothly through the stent. Follow-up esophagography revealed no in-stent stenosis and the silica gel membrane of the esophageal stent was stable in all stents.

Histological examination

HE staining revealed significant esophageal wall remodeling in the PP-silicone stent group compared to the control group. We did not find any obvious inflammatory cell infiltration in the submucosal layer from the sections. PCNA-positive cells (squamous epithelial cells) were mainly found in the epithelial layer; squamous epithelial cells located near the lumen and close to the stent were mostly negative for PCNA. Quantitative analysis of the PCNA-positive cells revealed no significant difference in proliferation index between the two groups (34.6 ± 0.4 % vs. 33.4 ± 0.6 % in control, $P > 0.05$). The epithelial layer, as measured on PCNA staining, was much thinner in the stent group than in the control group (111.4 ± 32.5 μm vs. 239.5 ± 17.2 μm; $P < 0.05$). However, the thickness of the epithelial layers did not differ between different follow-up time points in the PP-silicone stent group ($P>0.05$) (Fig.5). Masson staining showed that the submucosal collagen fiber deposition percentage in the PP-silicon-1w, PP-silicon-4w, and the control groups were 23.5 ± 0.3 %, 22.5 ± 0.8 % and 22.2 ± 0.3 %, respectively, which had no significant difference ($P > 0.05$) (Fig. 6).

Discussion

In this experiment we determined the tissue response and feasibility of a PP-silicone stent insertion into the normal esophagus of rabbits. We systematically evaluated the biomechanical properties of the PP esophageal stent with knitted PP fiber skeleton, the safety of the rabbit esophagus after internal stent expansion, and the performance of the stent. After subsequent analysis the data showed that polypropylene as a skeleton fiber knit esophageal stent for treatment of esophageal benign stricture is feasible and effective.

In recent years, there has been an increase in research interest in the treatment of esophageal benign strictures and a number of scholarly articles have been published on novel methods of temporary stenting.[23-25] Temporary stent therapy

has the advantages of being minimally invasive, safe, effective, and less likely to result in complications, especially for esophageal benign strictures.[26] Initially, the treatment of esophageal benign strictures utilized an uncovered membrane or partially covered membrane stent. Although in a retrospective analysis, the rate of complications occured in about 80% of patients, with new stricture formation accounting for 41%, stent migration accounted for 31%, pain or reflux accounted for 21%, and fistula formation accounted for 6%.[27,28] Moreover, metal stents cause tissue granulation and tissue hyperplasia, as a result of contact between the mucosa and the exposed metal stents,[29,30] the latter result is likely to again stricture. In addition, the disadvantages of metal stents include removal; if the stent is forcibly removed, the patient is likely to suffer an esophageal rupture. [31] Our previous studies have confirmed that metal stent insertion alone is likely to cause esophagus damage that triggers collagen synthesis.[9,18] A PP-Silicone-coated stent might cause less trauma to the esophagus wall than a metal stent, as its dilation strength is often gradual and less than metal stent. Moreover pp lines might be softer and more bio-compatible than a metal line, which means it is more likely to comply with esophageal mobility. However whether a PP-Silicone coated stent is effective to dilate esophagus stricture still needs further investigation.

Presently, there is still a common problem in the existing stent, which is reactive tissue hyperplasia on the top or bottom. The tissue hyperplasia often leads to the recurrence of dysphagia and stent blockage during removal.[32] Application of silica gel material and full membrane design can effectively reduce the reactive hyperplasia and tissue regeneration. Song et al.[33] have been reported to use new recyclable stent for esophageal stenosis and achieved good clinical efficacy in their results. However, a long-term study found that only a small portion of patients with dysphagia received prolonged remission, while a high proportion of patients emerged with stent translocation. [34] In short, temporary stent therapy has a certain positive effect, but restenosis, pain and other complications are still common after the operation. The optimal design of the temporary esophageal stent should be elastic, non traumatic, and with a certain diameter to ensure that the normal food can passed through. Moreover, good design should allow ease of insertion, reposition, and removal of the stent, and the stent should induce no displacement, tissue hyperplasia, or ingrowth risk.

Currently, there are two main categories of temporary esophageal stent supports which are: biodegradable stents and retrievable stents.[35] Stents with good biocompatibility and in vivo degradability have a temporary therapeutic effect. However, due to the expansion properties of the material, stents completely knitted from the degradable material have low tensile strength, are difficult to place, have weak curative effects, and are easily shifted.[36] On the other hand, retrievable stents often are constructed of metals. However, as most of the currently available stents are designed to be only concerned with stent removal, they are highly prone to displacement. [37,38] Over 50% of stent designs have been reported to displace during implantation.[39] Removable esophageal stents mainly consist of polymer coated metal stents fabricated from a layer of polymer coating over the metal stent. However, the limitations in this design include pain, perforation, bleeding, and a strong foreign body reaction caused by the late metal wire removal.

This experiment combined esophageal stent skeleton and tectorial membrane properties by selecting PP as a skeleton fiber knitted esophageal stent mould and fixing the support stent using biological medical silicone coating on the stent surface. The stent was designed by integrating the mechanical properties of metallic esophageal stents with the high expansion properties of the polymer in mind. After nearly 200 compressions, the material maintained its original mechanical compressive strength. This illustrates that the silicone-stabilized PP tubular stent can maintain its mechanical properties and structural stability. High tensile strength (around 6 MPa) and high tensile elongation (nearly 80%) were demonstrated in the mechanical analysis of the PP stent, and the stent section tensile test revealed that maximum tension the stent can withstand reaches 60 Newtons. The finite element simulation analysis of the whole stent showed that the left and right sides of the stent were also more obvious stress concentration as the loading contact site and the restrain site of the both ends. The stent demonstrated good elastic supporting force. It has also shown excellent recovery properties and the structural shape of the stent did not change during the implantation process. After 6 days of cultivation, PP-silicon shows negligibly different amounts of cell neumbers with the comparison group, and PP line has small difference in cell numbers compared with silicon membranes at 9 days of culture, which illustrates that PP-silicon can promote the inhibition of SMC cell growth.

The basic underlying concept of the treatment of benign esophageal stenosis is to tear the fibrous connective tissue or hyperplastic smooth muscle layer and provide enough support until the esophageal wall has healed. On this experiment we found that the epithelial and SMA layers had already stretched and become much thinner at 1 and 4 weeks indicating that the remodeling process had been completed. The other pathological findings, including inflammation on HE staining and esophageal wall injury assessed using PCNA staining of the epithelial layer and submucosal collagen deposition, revealed that the PP-silicone stent insertion had a slight reaction with surrounding tissues and the mucous membrane.

Based on this study, we aimed to demonstrate that the PP-silicon stent has a high value. Silicone has excellent elasticity, coating properties, and is resistant to in vivo degradation. Compared with other stents, PP fibers were used as rigid stent struts, and silicone membranes were used to cover the PP struts. This particular stent design demonstrated the following characteristics: 1) Flexible PP silk knitting provided good elasticity and self-expansion properties, which stabilized the expansion in the narrow place; 2) The stent has demonstrated a very strong radial support force and anti-pull force, which have been verified through in vitro experiments; 3) The membrane design can be adjusted if the supporting stent structure emerges during implantation.

There are no obvious complications such as esophageal stricture, perforation, bleeding or stent displacement in the experiment. In this experiment, the rate of stent displacement was low, but if a larger sample or longer observation time had been taken, the displacement rate may be higher.

This experiment has some limitations such as: The PP-silicone stent was inserted into the normal esophagus and the tissue reaction in the normal esophagus may differ from that in an esophageal stricture; short observation time so the recurrence case in the later period of the experiment and forward complications were observed less. This stent should be applied in a benign esophageal stenosis model to fully investigate its feasibility, efficacy, optimal implantation time and tissue reaction in vivo requires a longer follow-up study.

Conclusions

This experiment confirmed that our design of the PP-silicon stent achieved the properties of excellent tensile strength, good secureness, and few complications.

We believe that it can yield good treatment outcomes in benign esophageal stenosis mainly basing on pathological examination. The stent is unlikely to damage the esophagus, remains fixed in position, and the expansion of the stent persists over time. The operation is simple with strong controllability, thus the stent has high prospects for clinical application. It provides new stents for the treatment of benign esophageal stricture and a novel research path in the development of temporary stents in other benign strictures.

Acknowledgements

This work was supported in part by National Natural Science Foundation of China (51373112, 81171437, 81371659 and 81370041), Jiangsu Provincial Special Program of Medical Science (BL2012004), Jiangsu Provincial Clinical Orthopedic Center, the Priority Academic Program Development of Jiangsu Higher Education Institutions (PAPD).

References

1. Y. Q. Zhu, L. Edmonds, X. Zhao, X.L. Chen, C.M. Hu, Y.S. Cheng, W.G. Cui, *RSC Advances.*, 2014, **4**, 34405-34411.
2. R. Wirth, J Bauer, C. Sieber, *JPEN J Parenter Enteral Nutr.*, 2008, **32 (3)**, 285-287.
3. Y.Q. Zhu, Y.S. Cheng, G.Y. Tang, et al., *J Gastroenterol Hepatol.,* 2010, **25**, 499-505.
4. S. Jeon, S. Eun, C. Shim, C. Ryu, J. Kim, J. Cho, et al., *Endoscopy.,* 2009, **41**, 449.
5. J.C. Bakken, Kee. Wong, L.M. Song, P.C. Groen, T.H. Baron, *Gastrointest Endosc.,* 2010, **72,** 712-720.
6. M.A. Eloubeidi, T.L. Lopes, *Am J Gastroenterol.* 2009, **104,** 1374-1381
7. Y.Q. Zhu, Y.S. Cheng, M.H. Li, et al., *Neurogastroenterol Motil.*, 2010, **22,** 1240–1247 , e321-322.
8. F. Chung, S. Lin, C. Chou, H. Chen, C. Kuo, H. Lin, *Adv Biosci Biotech.,* 2013, **4,** 113–7.
9. U. Navaneethan, S. Duvuru, R Jagedeesan, et al., *Surg Endosc.,* 2014, **28**, 1194−1201.

10. F.J. Herth, S. Peter, F. Baty, R. Eberhardt, J.D. Leuppi, P.N. Chhajed, *Eur Respir J.,* 2010, **36,** 1370−1374.
11. M.M.C. Hirdes, F.P. Vleggaar, K. Linde, M. Willems, Willems, E. Willems, P.D. Siersema, *Endoscopy.,* 2011, **43,** 156–9.
12. M. Schweigert, M. Posada-Gozales, A. Dubecz, D. Ofner, H. Muschweck, H.J. Stein, *Interact Cardiovasc Thorac Surg.,* 2014, **18,** 190−196.
13. T.H. Kim, J.H. Shin, K.R. Kim, J.H. Park, J.H. Kim, H.Y. Song, *J Vasc Interv Radiol.,* 2014, **25,** 623−629.
14. Y.S. Cheng, F. Ma, Y.D. Li, N.W. Chen, W.X. Chen, J.G. Zhao,et al., *World J Gastroenterol: WJG.,* 2010, **16,** 5111.
15. M.T. McLoughlin, M.F. Byme, *World J Gastroenterol*., 2008, **14(24)**, 3798-3803.
16. A. Repici, F.P. Vleggaar, C. Hassan, et a1., *Gastrointest Endose*., 2010, **72,** 927-934.
17. X. Yu, L. Wang, M. Huang, et al., *J Msster Med*., 2012, **23 (2)**, 581-589.
18. Y.Q. Zhu, W.G. Cui, Y.S. Cheng, *Endoscopy*., 2013, **45(6),** 458-68.
19. Y.Q. Zhu, Y.S. Cheng, F. Li, M.H.; Li, J.G. Zhao, N.W. Chen, *Gastrointestinal . Endoscopy.,* 2011, **73(2),** 327-337.
20. W.G. Cui, L. Cheng, H. Li, Y. Zhou, Y. Zhang, J. Zhang, *Polymer.,* 2010, **51,** 2320–8.
21. W.G. Cui, Y. Zhou, J. Chang, *Sci Technol Adv Mater.,* 2010, **11,** 014108.
22. P. Gao, G.Z. Yan, Z.W. Wang, P.P. Jiang, H. Liu, *Int J Med Robotics Comput Assist Surg.,* 2012, **8,** 398-406.
23. J.G. Zhao, Y.D. Li, Y.S. Cheng, et al., *Eur Radiol.,* 2009, **19,** 1973–1980.
24. A.N. Holm, J.G. Mora,Levy, C.J. Gostout, M.D. Topazian, T.H. Baron, *Gastrointest Endosc*., 2008, **67(6),** 20-25.
25. P. Sharma, R. Kozarek, *Am J Gastroenterol.,* 2009, **105,** 258–73.
26. P.G .Van, Boeckel, F.P. Vleggaar, P.D. Siersema, *Clin Gastroenterol Hepat.,* 2011, **9**, 653-659.
27. M.A. Eloubeidi, J.P. Talreja, T.L. Lopes, B.S. Al-Awabdy, V.M. Shami, M. Kahaleh, *Gastrointest Endosc.,* 2011, **73,** 673-681.
28. U. Chaput, D. Heresbach, E. Audureau, G. Vanbiervliet, M. Gaudric, P. Bichard, P. Bauret, D. Coumaros, T. Ponchon, F. Fumex, E. Bensoussan, H. Lamouliatte,

A. Chryssostalis, F. Robin, F. Prat, *United European Gastroenterol J.*, 2013**, 1,** 93-102.

29. M.M. Hirdes, P.D. Siersema, F.P. Vleggaar, *Gastrointest Endosc*., 2012**, 75,** 712-718.
30. J.C. Bakken, Kee. Wong, L.M. Song, P.C. Groen, T.H. Baron, *Gastrointest Endosc.* , 2010, **72,** 712–720.
31. T. Thomas, K.R. Abrams, V. Subramanian, J. Mannath, K. Ragunath, *Endoscopy.,* 2011***, 43,*** 386-393.
32. D. J. Stewart, R. Balamurugan, N. J. Everitt, K. Ravi1, *Diseases of the Esophagus.,* 2013, **26,** 276–281.
33. J.H. Kim, J.H. Shin, Z.H. Di, G.Y. Ko, H.K. Yoon, K.B. Song, et a1., *J Vasc Interv Radiol*., 2005, **16(4)**, 543-548.
34. K.S. Dua, F.P. Vleggaar, R. Santharam, P.D. Siersema, *Am J Gastroenterol*., 2008, **103(12),** 2988-2994.
35. Z.H. Wang, N. Li, R. Li, Y.W. Li, L.Q. Ruan, *Materials International.,* 2014, **24,** 423–432.
36. F. Perez, Roldan, P. Gonzalez, Carro, M.C. Villafanez, Garcia, et al., *Endoscopy*., 2012, **44(3),** 297-300.
37. J.E. Van, Hooft, Berge. van, M.I. Henegouwen, E.A. Rauws, J.J. Bergman, O.R. Busch, P. Fockens, *Gastrointest Endosc.,* 2011, **73,** 1043-1047.
38. D.T. Dan, B. Gannavarapu, J.G. Lee, K. Chang, V.R. Muthusamy, *Diseases of the Esophagus*., 2012**, Nov,** 2:1–7.
39. M.A Eloubeidi, J.P. Talreja, T.L. Lopes, B.S. Al-Awabdy, V.M. Shami, M. Kahaleh, *Gastrointestinal Endoscopy*., 2011, **73(4),** 673–81.

Figure Legends

Fig. 1 (a) perfectly opened bare stents landscape and profile. (b) the relative data parameters of the stent; (c-f) the external stent in the push and release map in 8 mm (24 FR) delivery system.

Fig. 2 (a) horizontal radial elastic pressure detection and curve detection. The bracket can withstand the pressure and elastic changes. (b) a bracket section of tensile testing. The stress strain curves show the stent materials section can bear the pulling force.

Fig. 3 (a) the geometric model of the stent; (b) the mesh model of the stent; (c)stent stress distributions.

Fig. 4. CCK-8 assay of SMC proliferation on the PP line, silicon membranes and PP-silicon after 1, 3, 6 and 9 days of culture. TCP was set as control ($P > 0.05$) compared with PP-silicon stent.

Fig. 5 (a) Immunohistochemical staining for PCNA positive cells in the esophageal epithelial layer after inserting the stent at 1 and 4 weeks follow-up intervals; PCNA positive epithelial cells were observed in the esophageal epithelial layer (black arrows, magnification×400); Between the red lines was the thickness of esophageal epithelial layer. (b) At 1 week and 4 weeks after stent insertion, the epithelial tissue was significantly thinner in the PP-silicon stent groups than control ($P<0.05$); however, proliferation rate of PCNA positive epithelial cells were similar between PP-silicon stent groups and the control ($P>0.05$).

Fig. 6 Masson staining shows submucosal collagen fiber (blue arrows, magnification×400) deposition in the the control group (a), group PP-silicon-1w group (b) and PP-silicon-4w group (c). The percentage rate of collagen fiber deposition has no significant difference among the three groups ($P > 0.05$) (d).

Figures

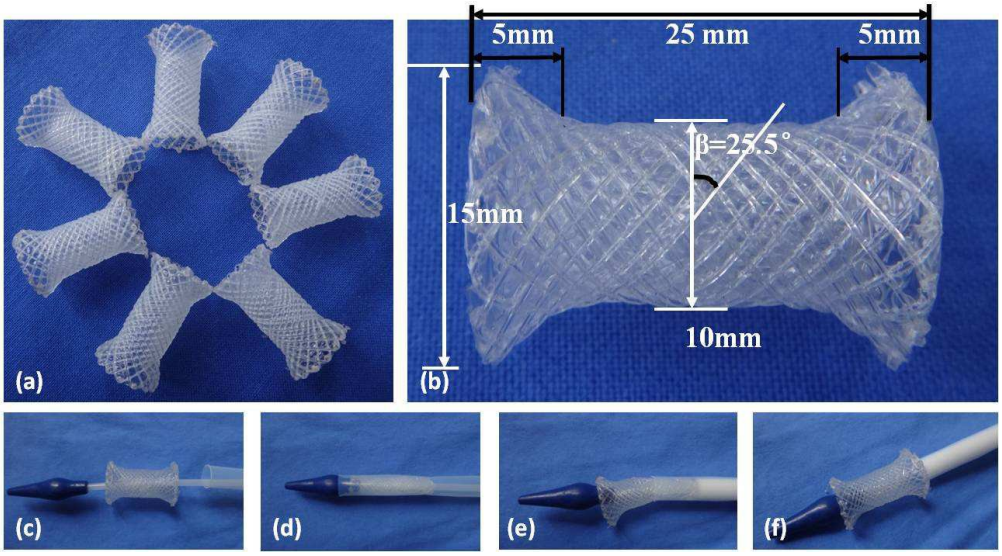

Fig. 1 (a) perfectly opened bare stents landscape and profile. (b) the relative data parameters of the stent; (c-f) the external stent in the push and release map in 8 mm (24 FR) delivery system.

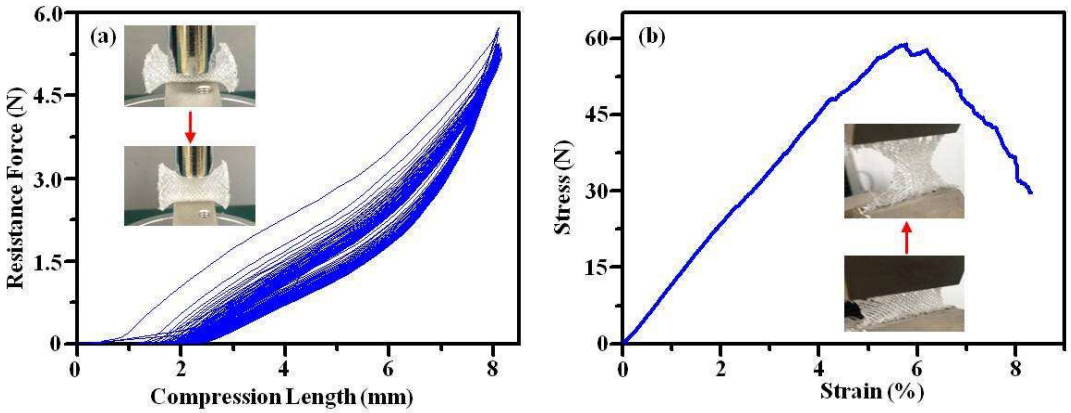

Fig. 2 (a) horizontal radial elastic pressure detection and curve detection. The bracket can withstand the pressure and elastic changes. (b) a bracket section of tensile testing. The stress strain curves show the stent materials section can bear the pulling force.

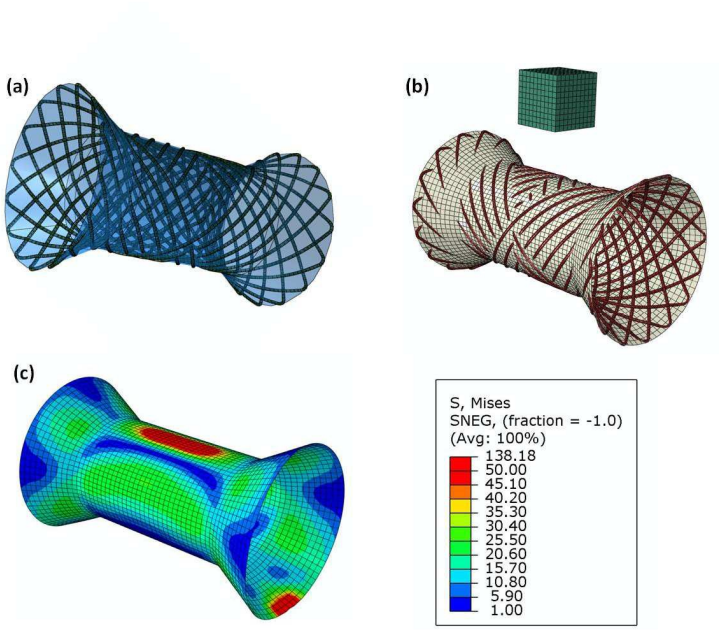

Fig. 3 (a) the geometric model of the stent; (b) the mesh model of the stent; (c)stent stress distributions.

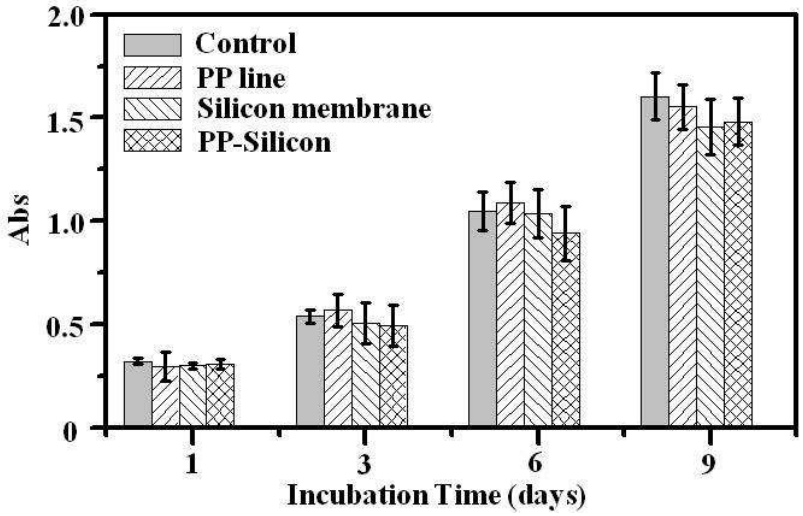

Fig. 4. CCK-8 assay of SMC proliferation on the PP line, silicon membranes and PP-silicon after 1, 3, 6 and 9 days of culture. TCP was set as control ($P > 0.05$) compared with PP-silicon stent.

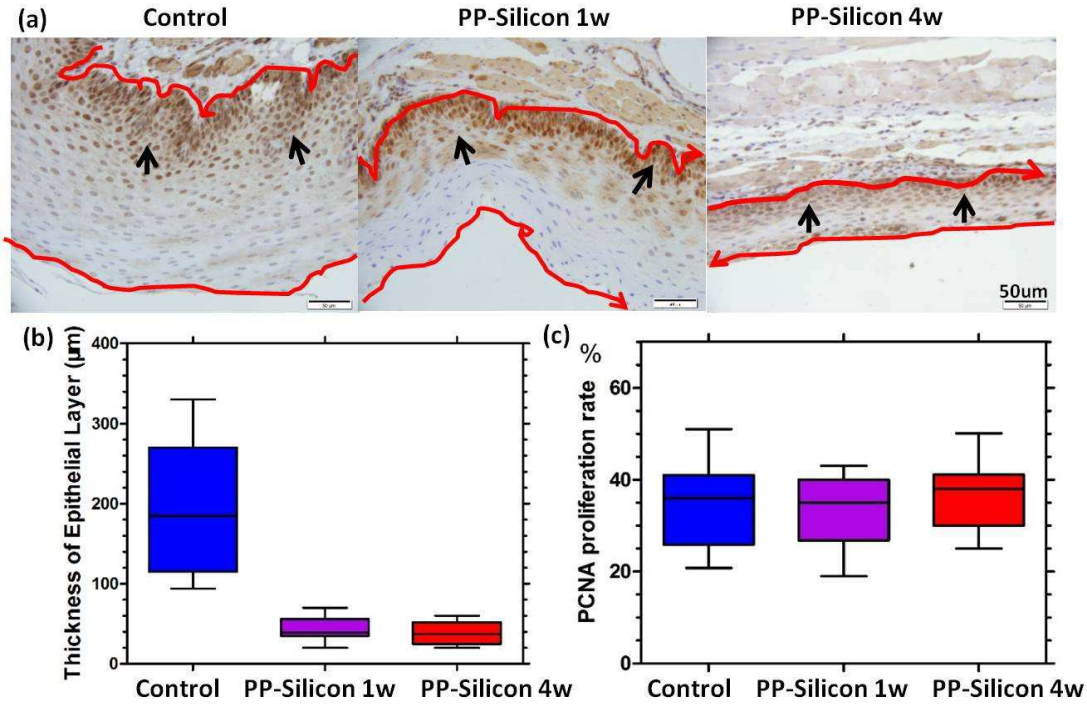

Fig. 5 (a) Immunohistochemical staining for PCNA positive cells in the esophageal epithelial layer after inserting the stent at 1 and 4 weeks follow-up intervals; PCNA positive epithelial cells were observed in the esophageal epithelial layer (black arrows, magnification×400); Between the red lines was the thickness of esophageal epithelial layer. (b) At 1 week and 4 weeks after stent insertion, the epithelial tissue was significantly thinner in the PP-silicon stent groups than control ($P<0.05$); however, proliferation rate of PCNA positive epithelial cells were similar between PP-silicon stent groups and the control ($P>0.05$).

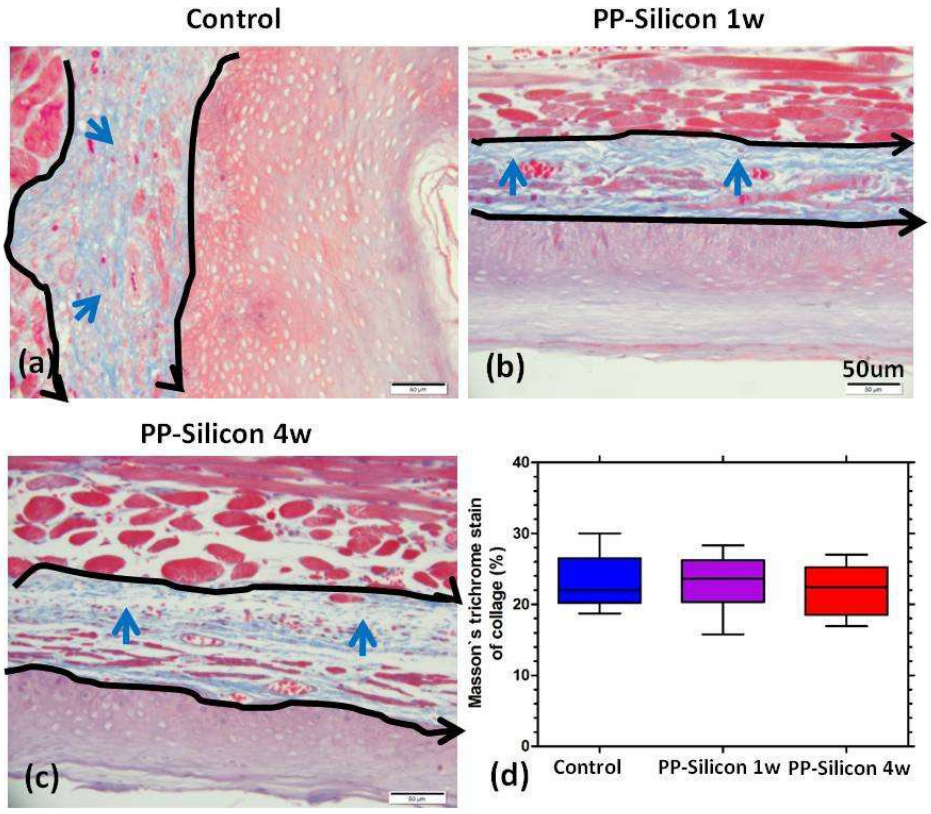

Fig. 6 Masson staining shows submucosal collagen fiber (blue arrows, magnification×400) deposition in the the control group (a), group PP-silicon-1w group (b) and PP-silicon-4w group (c) . The percentage rate of collagen fiber deposition has no significant difference among the three groups (P > 0.05) (d).

Graphic for manuscript